of vasopressin [8] or aldosterone [5], and various procedures to elicit inner ear autoimmune disease [4,9]. Recently, the two-phase hydrops guinea pig model has been developed [5]. This is based on a combination of chronic ES dysfunction, induced by mild destruction of the most distal part of the ES, and acute stress-induced endolymph production by stimulating Na/K-ATPase in stria vascularis, using aldosterone. However, this model still showed no vestibular dysfunction.

At this point, the question arises: 'What is the cause and pathogenesis of MD, and especially of vertigo'? There are no conclusive answers to this question; at least, EH alone is not enough to explain the episodic vertigo. There must be other factors.

More recently, we have succeeded in inducing EH in mice without recourse to any surgical procedure on the ED and ES. We combined overproduction of endolymph with reduced absorption of endolymph (or ES dysfunction) to induce EH. We also succeeded in inducing reversible vestibular dysfunction in our animal model by injecting epinephrine into the middle ear cavity [10]. However, the precise mechanism of this vestibular dysfunction and the relationships between the vestibular dysfunction of our model and the episodic vertigo in MD patients are still obscure. The purpose of the present study was to reveal the mechanism of vestibular dysfunction in our mouse model, which will give us more complete knowledge concerning the pathogenesis of MD.

## Materials and methods

Twenty-eight adult CBA/J mice, of 20–25 g body weight and with a normal Preyer's reflex, were used in this study. The care and use of the animals was approved by the Animal Experimentation Committee, Hiroshima University School of Medicine (permit no. A06-68) and was in accordance with the Guide to Animal Experimentation, Hiroshima University and the Committee on Research Facilities for Laboratory Animal Science, Hiroshima University School of Medicine.

The MD model was devised according to our original method, described in an earlier paper [10]. Briefly, mice were inoculated once daily for 5 days with 1 mg lipopolysaccharide (LPS) extracted from Escherichia coli (Sigma Chemical Co., St Louis, MO, USA) dissolved in 0.1 ml of sterile saline. LPS was instilled into the left tympanic cavity through the tympanic membrane via a sterile 27-gauge needle. At the same time, the mice were also given a daily intraperitoneal injection of aldosterone at a dose of 100 μg/100 g/day (Acros Organics, New Jersey, USA) for 5 days.

At 24 h after the last injection, 1:10 000 epinephrine or 3% sodium nitroprusside (SNP) was injected into the middle ear cavity through a tiny puncture in the posterior-inferior quadrant of the tympanic membrane of the left ear of the (normal) control and model animals [11]. The mice were sacrificed under deep anesthesia with pentobarbital and fixed by cardiac perfusion with 4% paraformaldehyde in 0.1 M phosphate buffer solution, pH 7.4, at the following times: 2 h after instilling epinephrine or 1 h after SNP. These periods were selected to induce the maximum reaction in the ES, as in our previous investigation [11]. The temporal bones were excised and immersed in the same fixative for another 2 h. They were decalcified with 0.1 M buffered Na-EDTA for 14 days. The specimens were then dehydrated with graded ethanols and embedded in a water-soluble resin (JB-4®). Sections were cut about 4 μm thick and stained with toluidine blue for light microscopy.

The light microscopic specimens were viewed in a Nikon photomicroscope (Eclipse E600). Analog images were obtained using an intensified digital color charge-coupled device camera (C4742-95; Hamamatsu Photonics) and stored as digital images using IP Lab Spectrum software (version 3.0; Signal Analytics Corporation).

### *Quantitative assessment of changes in endolymphatic space in cochlea*

For quantitative assessment of the changes in the endolymphatic space, the ratios of the change in length of Reissner's membrane and the cross-sectional area of scala media were measured in mid-modiolar sections of the cochlea, according to the method described by Kakigi et al. [12]. In principle, one specimen was used for the analysis of one cochlea. Sections cut closest to the mid-modiolar plane in individual turns were used. For this analysis, the following four parameters were measured in the lower and upper turns, not including the hook portion: 1) the length of the extended Reissner's membrane (L); 2) the ideal length of Reissner's membrane (L*); this segment represents the normal position of the idealized Reissner's membrane, which connects the normal lateral attachment of Reissner's membrane at the upper margin of stria vascularis to its normal medial attachment at the spiral limbus; 3) the cross-sectional area of scala media (S), enclosed by the distended Reissner's membrane; and 4) the cross-sectional area of the original scala media (S*), enclosed by a straight line segment. The anatomical measurements were carried out in 'blind' fashion using IP Lab Spectrum software. From these parameters, the increasing ratio (%) between the length of Reissner's membrane (IR-L) and the cross-sectional

area of the S (IR-S) of an upper or lower turn was calculated according to the equation described below.

$$IR\text{-}L = 100 \times Lx/L^*x \text{ (x: upper or lower turn)}$$

$$IR\text{-}S = 100 \times Sx/S^*x \text{ (x: upper or lower turn)}$$

*Quantitative assessment of changes in endolymphatic space in vestibule*

For the quantitative assessment of changes in the endolymphatic space in the vestibule, the relative sizes of this space in the cross-sectional area of the utricle, saccule, and posterior ampulla were measured. In principle, one specimen was used to analyze one vestibule. One light micrograph from the stored digital images was prepared from the sections including stapes, utricle and saccule, or from the sections cut at the mid-portion of the posterior crista ampullaris. To analyze utricle and ampulla, the endolymphatic space and the bony lining of the vestibule were outlined on these photographs. The relative size of the endolymphatic space, as compared with the bony lining of the vestibule, was calculated using IP Lab Spectrum software.

To analyze the saccule, the following two parameters were measured: 1) the cross-sectional area of the endolymphatic space (S), enclosed by the saccular wall; and 2) the cross-sectional area of the hypothesized original saccular wall (S*), enclosed by a straight line segment attached to the bony wall. The anatomical measurements were carried out using IP Lab Spectrum software. From these parameters, the relative size (%) of the endolymphatic space of the S could be calculated (Figure 1).

*Quantitative assessment of luminal size change in ES*

The sizes of the ES lumen in the intra-osseous rugose portion as well as in the extra-osseous distal portion were calculated in the following way [10]. One light micrograph from the stored digital images was prepared from the mid-portion of the intra-osseous rugose portion of each ES. On these photographs, the lumen of the sac and the bony lining of the vestibular aqueduct were outlined. The relative size of the lumen as compared with the bony lining of the vestibular aqueduct was calculated (IP Lab Spectrum software). In the distal portion of the ES, one light micrograph from the stored digital images was prepared at the distal portion of each ES. On these photographs, the short diameter of the lumen of the sac and that of the outer lining of whole ES were measured. The relative diameter was calculated again (IP Lab Spectrum software) [4,7].

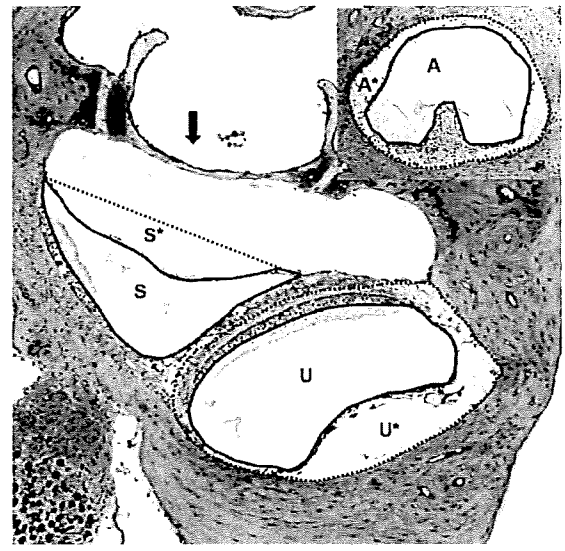


Figure 1. Quantitative assessment of changes in the endolymphatic space in the vestibule. The ratios of the change in cross-sectional area of the utricle (U), saccule (S), and posterior ampulla (A) were determined. To analyze the utricle and ampulla, the endolymphatic space (U, A) and bony lining of the vestibule (U*, A*) were outlined. To analyze the saccule, the following two parameters were measured: 1) the cross-sectional area of the endolymphatic space (S), enclosed by the saccular wall; and 2) the cross-sectional area of the hypothesized original saccular wall (S*), enclosed by a straight line segment attached to the bony wall. From these parameters, the relative ratios (%) of the cross-sectional area of the U, A, and S were calculated (relative ratio (%) = U/U*, = A/A*, = S/S*). Arrow, stapes.

## Results

*Behavioral data*

Treatment of the model animals with epinephrine induced signs of vestibular dysfunction. The vestibular effects started to appear within 5 min. In the most affected stage, the animals could not maintain a stable posture but leaned to the left (injected) side. They were unable to swim and when walking showed a tendency to turn to the left. At the same time, faint but distinct nystagmus toward the right (non-injected) side was noted. In contrast, treatment with SNP did not induce any behavioral changes [10].

*Cochlea*

The morphological changes following treatment of normal mice with epinephrine or SNP were described in detail in our previous paper [11]. Briefly, in the stria vascularis, intercellular spaces displayed expansion with abundant vacuolar formation 2 h after the topical application of epinephrine. In contrast, topical SNP did not induce such morphological changes in the stria vascularis after 1 h. Also in contrast to the morphological changes in the stria vascularis, there

were no signs of EH or collapse of Reissner's membrane in either group.

In the ears of model mice, all cochleas showed mild to moderate EH. Intracochlear variation was observed in the severity of hydrops (Figure 2a). The severity of hydrops was generally greater in the upper turn of the cochlea. After topical application of epinephrine in the model animals, the stria vascularis showed expansion of the intercellular spaces, with abundant vacuolar formation. Topical application of SNP also elicited expansion of the intercellular spaces, although less than observed after the application of epinephrine and similar to that in the model animals. After the epinephrine injection, elongation and folding of Reissner's membrane was marked, especially in the lower turn, resulting in alleviation of EH (Figure 2b). On the other hand, application of SNP did not induce such morphological changes. The cochleae showed mild to moderate EH. Folding of Reissner's membrane was not observed (Figure 2c).

The increasing ratio of the length of Reissner's membrane (IR-L) vs the cross-sectional area of scala media (IR-S) in the upper and lower turns was calculated in the model animals. IR-S was $131 \pm 8.4\%$ (mean $\pm$ SD, $n = 5$) (upper turn) and $123 \pm 3.2\%$ (lower turn); IR-L was $117 \pm 9.0\%$ (upper turn) and $120 \pm 15.9\%$ (lower turn). After the injection of epinephrine, IR-S decreased significantly to $114 \pm 15.3\%$ ($n = 4$) (upper turn) and $113 \pm 5.4\%$ (lower turn) ($p < 0.05$, Student's $t$ test), while IR-L showed no significant differences, i.e. $119 \pm 15.3\%$ (upper turn) and $120 \pm 10.6\%$ (lower turn). In the SNP-treated ears, IR-S was $128 \pm 7.8\%$ ($n = 4$) (upper turn) and $119 \pm 5.8\%$ (lower turn), and IR-L was $118 \pm 8.3\%$ (upper turn) and $118 \pm 13.5\%$ (lower turn); these showed no significant differences (Figure 3).

*Vestibular parts*

Topical application of SNP or epinephrine in the normal mice did not induce any morphological

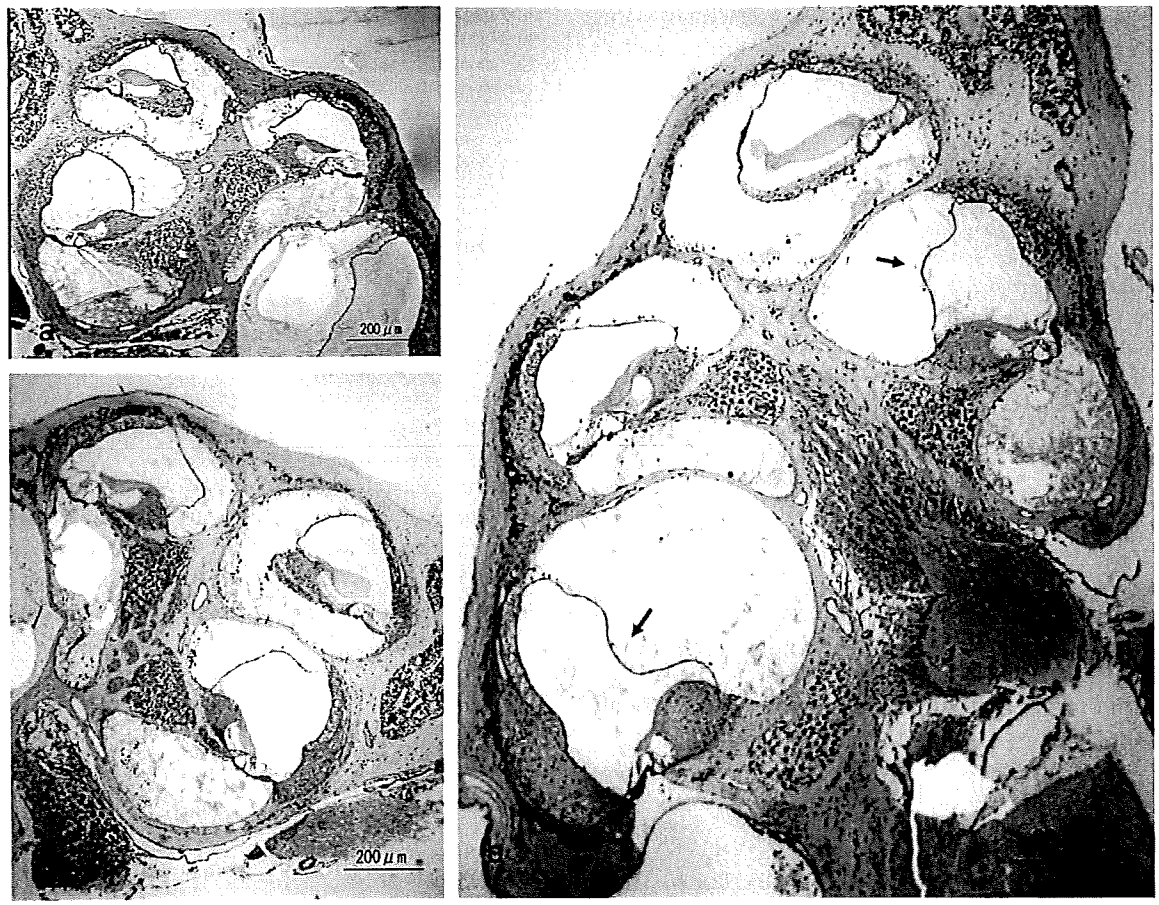


Figure 2. (a) In the ears of 'model' mice, cochleae show mild to moderate endolymphatic hydrops (EH). (b) After topical application of epinephrine, elongation and folding of Reissner's membrane was marked (arrows), especially in the lower turn, resulting in a reduction of EH. (c) Sodium nitroprusside (SNP) did not induce such morphological changes. The cochleae showed mild to moderate EH.

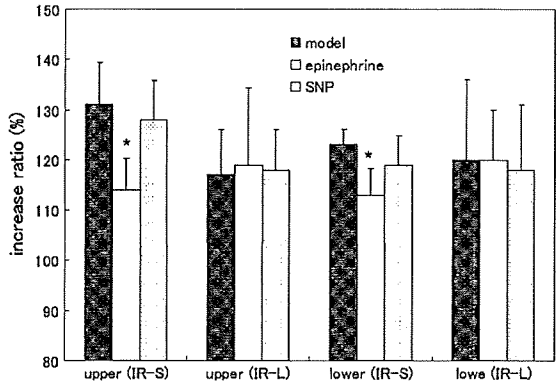


Figure 3. The increasing ratios of the length of Reissner's membrane (IR-L) and the cross-sectional area of scala media (IR-S) in the upper and lower turns was calculated in the model animals. After the injection of epinephrine, IR-S was significantly decreased in the upper and lower turns, while IR-L showed no significant differences. In the SNP treated ear, IR-S and IR-L showed no significant differences. $*p<0.05$.

changes in the utricle, saccule, or ampulla, such as collapse of the endolymphatic space or EH.

In the ears of model animals, all vestibular parts failed to show signs of EH, in contrast to the mild or moderate EH in the cochlea (Figure 4a, c). After topical application of epinephrine in the model animals, a mild increase in the endolymphatic space (EH) was observed in the utricle, the ampulla, and (strongest) in the saccule (Figure 4b, c).

In normal ears, the relative luminal size of the endolymphatic space was determined in the utricle ($52\pm10.5\%$, mean $\pm$SD, $n=5$), saccule ($82\pm7.7\%$), and posterior ampulla ($57\pm6.2\%$). After treatment with epinephrine (normal mice, $n=5$), the relative sizes were as follows: in the utricle, $50\pm12.5\%$; saccule, $80\pm5.1\%$, and ampulla, $56\pm8.5\%$. After the treatment of normal mice ($n=5$) with SNP, the relative size of the endolymphatic space was $54\pm13.5\%$ in the utricle, $83\pm10.1\%$ in saccule, and $56\pm10.0\%$ in the ampulla. Neither treatment revealed any significant difference.

In the model animals, the corresponding sizes were: $58\pm4.2\%$ ($n=5$) in the utricle, $85\pm7.4\%$ in the saccule, and $62\pm12.4\%$ in the ampulla, showing no significant difference vs normal mice. After the treatment of model mice ($n=4$) with epinephrine, the relative size of the endolymphatic space was significantly increased, to $69\pm2.1\%$ in the utricle ($p<0.01$), $125\pm12.4\%$ in the saccule ($p<0.01$), and $71\pm8.9\%$ in the ampulla ($p<0.05$). After the treatment with SNP ($n=4$), the corresponding measurements were: $60\pm3.7\%$ in the utricle, $83\pm4.1\%$ in the saccule, and $65\pm5.3\%$ in the ampulla, showing no significant differences (Figure 5).

### *Endolymphatic sac*

The ED and ES were both studied histologically. In the control ears, the intra-osseous portion of the ES was easily identified by virtue of its cylindrical cells, which protrude into the lumen as irregular papillae. Numerous distended lateral intercellular spaces (LIS) were seen in the epithelial cell lining of the ES. The epithelial cells were columnar in general (Figure 6a). In the distal portion of the ES, LIS were not so distended as in the intra-osseous portion, but were nevertheless evident. The epithelial lining of the distal portion of the ES was cuboid, except at the extreme end, where it was squamous.

After treatment of control mice with epinephrine, the lumen of the distal portion of the ES was narrower and had collapsed. Distended LIS were observed between the cuboid epithelial cells. Inside the lumen, a number of macrophages were observed. In the intra-osseous portion of the ES, the lumen of the ES had

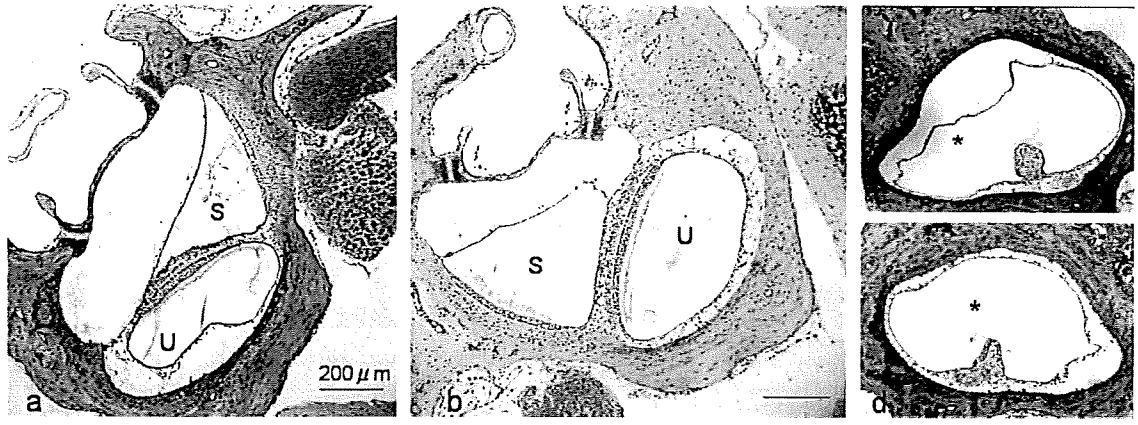


Figure 4. (a, c) In the ear of a model animal, all vestibular parts revealed no signs of endolymphatic hydrops (EH). S, saccule; U, utricle; *, ampulla. (b, d) After topical application of epinephrine to the model animals, mild EH was observed in the utricle (U) and ampulla (*), and was strongest in the saccule (S).

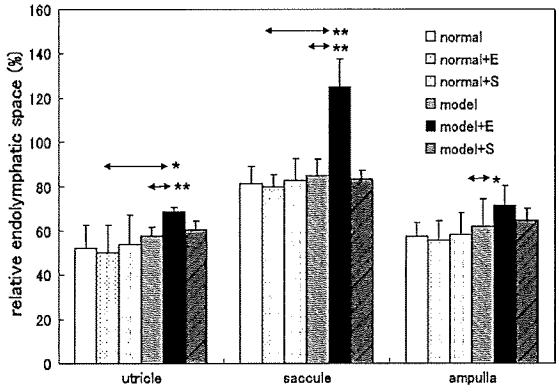


Figure 5. The relative luminal sizes of the endolymphatic space were determined in the utricle, saccule, and posterior ampulla. After treating normal mice with epinephrine or SNP, the relative size of the endolymphatic space showed no significant difference. After treatment of model mice with epinephrine, the relative size of the endolymphatic space was significantly increased in the utricle ($p < 0.01$), saccule ($p < 0.01$), and ampulla ($p < 0.05$). After treating model mice with sodium nitroprusside (SNP), the relative size of the endolymphatic space showed no significant difference.

collapsed and contained a stainable substance. The LIS looked distended and were generally larger. At the same time, so-called granular cells were observed with a rich content of stainable granules in the cytoplasm (Figure 6b).

In the SNP-treated ears, the lumen of the distal portion of the ES was noticeably dilated. The epithelial cells had become thinner and the LIS had collapsed. Inside the lumen, the ES contained clear endolymph without macrophages. The intra-osseous portion of the ES was also dilated. The LIS had also collapsed and the looseness of the perisaccular tissue was not observed. The epithelial cells were often cuboid or of flat type. The granular cells were not observed in general (Figure 6c).

In the model mice, the morphological features of the ES differed considerably. The distal portion of the ES showed wide variations, from near collapse to marked dilation. The LIS appeared generally distended. The intra-osseous portion of the ES showed a wide variation too, while the ES lumen was generally slightly dilated. The LIS were generally distended. Granular cells were observed in some specimens.

After the injection of epinephrine in the model mice, the ES lumen was also slightly dilated, while granular cells were observed in some specimens (Figure 3d). After the SNP injection, the ES did not show dilation of the lumen or collapse of the LIS. In general, no granular cells were observed (Figure 3e).

The relative luminal size of the ES was determined using the ratio between the size of the ES lumen and

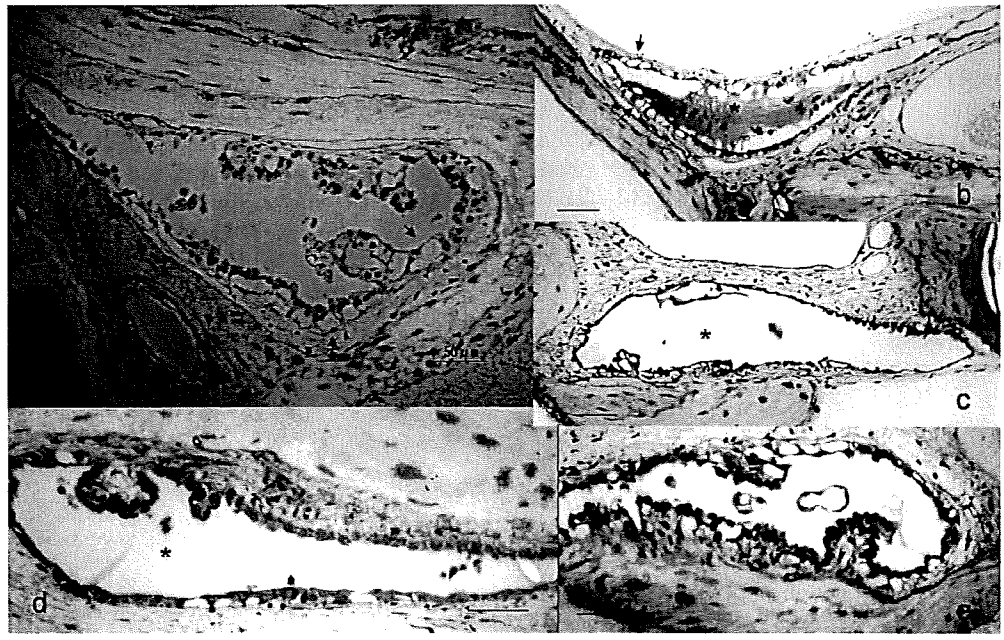


Figure 6. (a) In the control ears, the intra-osseous portion of the endolymphatic sac (ES) was easily identified by its cylindrical cells, which protruded into the lumen as irregular papillae. In the intra-osseous portion of the ES, numerous distended lateral intercellular spaces (LIS) were seen in the epithelial cell lining of the ES (arrows). The epithelial cells were generally columnar. (b) In the epinephrine-treated ears, the lumen of the ES had collapsed and contained a stainable substance (asterisk). The LIS appeared distended, showing a general increase in size (arrows). (c) In the sodium nitroprusside (SNP)-treated ears, the lumen of the intra-osseous part of the ES was dilated (asterisk). The LIS had collapsed and looseness of the perisaccular tissue was not observed. (d) After the injection of epinephrine in the model mice, the ES showed slight dilation of the lumen (asterisk). (e) After the SNP injection, the ES did not show either dilation of the lumen or collapse of the LIS.

that of the bony vestibular aqueduct in the intermediate, rugose portion as well as the ratio between the ES lumen diameter and that of the whole ES in the distal portion. In normal ears, the luminal size of the ES was 68±3.5% (mean±SD, $n=5$) in the distal part and 47±2.2% in the intra-osseous portion. After the treatment of normal mice ($n=5$) with epinephrine, the luminal size of the ES was 64±4.7% in the distal part and significantly ($p<0.05$) reduced to 36±9.5% in the intra-osseous portion. After the treatment with SNP ($n=5$), the luminal size of the ES was significantly increased ($p<0.01$) to 83±3.4% in the distal part and 68±4.7% in the intra-osseous portion after 1 h.

In the model animals, the luminal size of the ES was 72±11.2% ($n=5$) in the distal part and 43±4.0% in the intra-osseous portion. After the epinephrine treatment ($n=4$), the size of the ES lumen was 85±1.3% in the distal part and was significantly ($p<0.05$) increased to 59±11.7% in the intra-osseous portion. After treatment with SNP ($n=4$), the ES lumen was 72±4.3% in the distal part and 37±4.6% in the intra-osseous portion, i.e. no significant differences (Figure 7).

## Discussion

Numerous investigators have suggested that the symptoms of MD derive from a disturbance in the volume/pressure relationship in the endolymph. It is not yet known whether hydrops is the cause of the symptoms or merely a side effect of the disorder. Actually, MD patients never suffer from incessant vertigo. Typically, the vertigo begins quite suddenly and intensifies over minutes or hours and when severe, nausea and vomiting may ensue. As movement during vertigo exacerbates the nausea, patients soon learn to stay motionless during an attack. The vertigo usually lasts more than 20 min, but rarely more than 24 h. Vertigo attacks occur episodically, triggered by additional factors such as emotional stress [4]. In human temporal bone studies, EH has been observed in the temporal bones of persons showing symptoms and signs of MD [13–15]. Indeed, hydrops is both the histological hallmark of MD and the working concept of its pathogenesis. Paradoxically, not all people with symptoms of MD have hydrops, and not all people with hydrops discovered at autopsy had symptoms during life [15].

Even though obliteration of the ED and ES is ideally the most readily available procedure for producing hydrops, this model is not perfect for MD, because after such procedures the guinea pig rarely shows episodic vestibular symptoms [2–4]. Although it is being extensively studied, the standard guinea pig model does not reliably reproduce vestibular symptoms. Importantly, hydrops is produced by underresorption of the endolymph, a mechanism that might not directly resemble the production of hydrops in MD [2–4]. Other induced models, e.g. delayed perilymphatic infusion of keyhole limpet hemocyanin [9], anti-CB11 monoclonal antibodies, cholera toxin [7], chronic administration of vasopressin [8], the

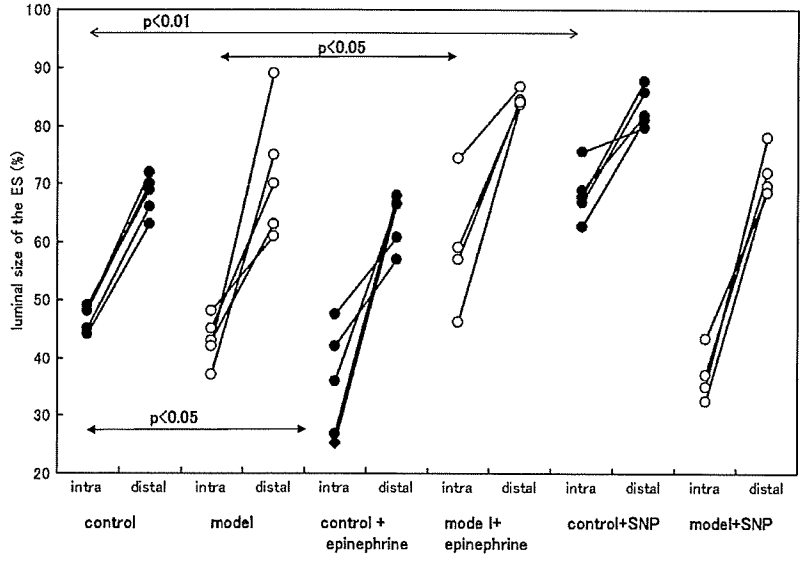


Figure 7. The relative luminal size of the endolymphatic sac (ES) was determined. After normal mice were treated with epinephrine, the size of the ES lumen was reduced in the intra-osseous portion, whereas after treatment with sodium nitroprusside (SNP) it was significantly increased in both the distal part and the intra-osseous portion. After the model animals were treated with epinephrine, the size of the ES lumen was increased in the intra-osseous portion, while after treatment with SNP, it showed no difference.

two-phase hydrops guinea pig model [5], and our new model [10] all appear to have the same limitations inherent in the standard guinea pig model. Based on the present and previous investigations, it is speculated that vestibular dysfunction may not result from the existence of EH alone. In another way, all animal models (including our new model) might be a model of an asymptomatic period of MD [10]. Based on this hypothesis, we thought that vestibular dysfunction could be induced by some additional stress. It is well known that the dysfunction of the ES is closely related to vestibular dysfunction. It has been reported that pretreatment with colchicine reduced or inhibited the glycerol-induced secretion of macromolecules in the ES. The lumen collapsed, but often there was no presence of stainable substance [16]. The secretory activity in the ES may be closely related to the regulation of inner ear fluid homeostasis, and functional disturbances in this system can lead to disorders of inner ear function [16,17]. Animals treated with colchicine showed pronounced signs of inner ear malfunction after the additional systemic glycerol administration, which could indicate that rapid volume reduction of endolymph (additional stress) can cause vestibular dysfunction if the ES function has previously been impaired [16]. Similar reversible vestibular dysfunction was noted after systemic administration of glycerol in a surgical obliteration model in the guinea pig [18]. The animals used in that study had not yet reached an EH, representing only loss of normal ES functions, as they were used immediately after surgical destruction of the ED and ES. Under such conditions without EH but with loss of ES function, the glycerol treatment induced reversible vestibular dysfunction. These findings may mean that the ES actually compensates the sudden reduction in endolymphatic volume and/or pressure.

We have to consider the factors needed to induce vestibular dysfunction in hydropic animals. The present study revealed that topical injection of epinephrine caused vestibular dysfunction, whereas topical injection of SNP did not elicit any such signs. Epinephrine applied topically (1:10 000) to the round window membrane caused an immediate reduction of inner ear blood flow (IBF) (mean reduction 60%, maximum peak reduction 65–85% across subjects), which recovered slowly ( >10 min) toward baseline following removal of epinephrine [19]. In contrast, topical application of 3% SNP induced a rapid (within 10 min) and noticeable increase in IBF (more than double). There was no obvious recovery from this topically induced change during the entire duration of the experiment (2 h) [20]. It is thus shown that the reduction in IBF could be used to exert additional stress to induce vestibular dysfunction in our model animal, whereas an increase in IBF could not. Reduced IBF induced a reduction in endolymph volume, whereas an increase of IBF increased it [11]. Similarly, glycerol administration can reduce the volume and/or pressure of endolymph, causing vestibular dysfunction in animals lacking normal ES function [16]. From these findings, we conclude that a reduction in endolymph volume and/or pressure induced by a variety of causes such as decreased IBF, glycerol, and other possible factors, can be used as an essential additional stress to induce vestibular symptoms in hydropic model animals.

Other important factors were the functions of the ES as well as the reactions of vestibular parts. We reported earlier that topical application of epinephrine or SNP in normal animals did not induce any signs of vestibular dysfunction or of EH [11]. The present investigation has also revealed that topical application of epinephrine or SNP did not elicit any signs of EH or collapse of the endolymphatic space in the vestibular parts, whereas the ES showed a marked reaction. Topical application of epinephrine led to a decrease in or partial collapse of the ES lumen, accompanied by enlargement of the LIS, and deposition of a stainable substance in the lumen. Similarly, topical application of SNP also led to an increase in the size of the ES lumen, but accompanied by collapse of the LIS and dense perisaccular tissue. This may mean that the ES actively regulates the inner ear fluid homeostasis during sudden changes in IBF [11]. It is therefore suggested that the volume and/or pressure in the inner ear is strictly regulated by the local regulatory system and/or by the dynamic functioning of the ES.

The present investigation revealed that topical injection of epinephrine in model animals caused a marked elongation and folding of Reissner's membrane, especially in the lower turn, resulting in alleviation of EH. The degree of EH was significantly reduced, but the length of Reissner's membrane was unchanged. On the other hand, the application of SNP did not induce such morphological changes. In the vestibular parts (i.e. utricle, saccule, and ampulla) the endolymphatic space expanded, showing signs of EH after the administration of epinephrine. The ES too showed the same abnormal reaction. After application of epinephrine in the model animals, the lumen of the ES was slightly dilated, in contrast to the partial collapse of the lumen in the normal ES. These findings mean that the regulatory functions of endolymph fluid volume and/or pressure in the vestibule and ES were lost in our new model. Thus, the model animals could not compensate for the rapid reduction of endolymph volume and/or pressure, and probably not for the rapid ionic imbalance either, resulting in vestibular dysfunction following additional stress.

Thus, the normal ES function that regulates inner ear fluid homeostasis was lost in our model.

To sum up, inner ear fluid homeostasis is strictly regulated in untreated animals. When the IBF is increased, the endolymphatic volume also increases, regulated by expansion of the ES lumen. But when the IBF is reduced, the endolymphatic volume decreases, regulated by the collapse of the ES lumen and subsequent secretion of stainable substance. After treatment with both aldosterone and LPS (model animal), the endolymph volume increases and the absorption of endolymph decreases. The functioning of the ES is impaired. When the IBF is increased in the model animals, there may be no obvious changes in the inner ear, but when it is reduced, the endolymph volume in the cochlea is also reduced, resulting in folding of Reisner's membrane. The vestibular part represents the increased EH, which can cause rapid ionic imbalance, resulting in pronounced vestibular dysfunction. The ES also revealed an abnormal reaction, showing an expansion of the ES lumen (Figure 8).

Based on our previous studies and the present investigation, we consider the pathogenesis of MD as follows. EH is caused by several extrinsic and intrinsic factors [15]. These include hypoplasia of the vestibular aqueduct and sac, racial genetic factors, autoimmunity, otitis media, trauma, otosclerosis, vasopressin, allergy, and viral infection. Patients with EH alone do not generally suffer from vertigo. However, additional stress such as sudden changes in endolymphatic pressure, restricted IBF, rupture of the endolymphatic membrane (Reissner's or the saccular wall), can cause a vertigo attack. It seems logical that both physical and chemical mechanisms can concomitantly cause the symptoms.

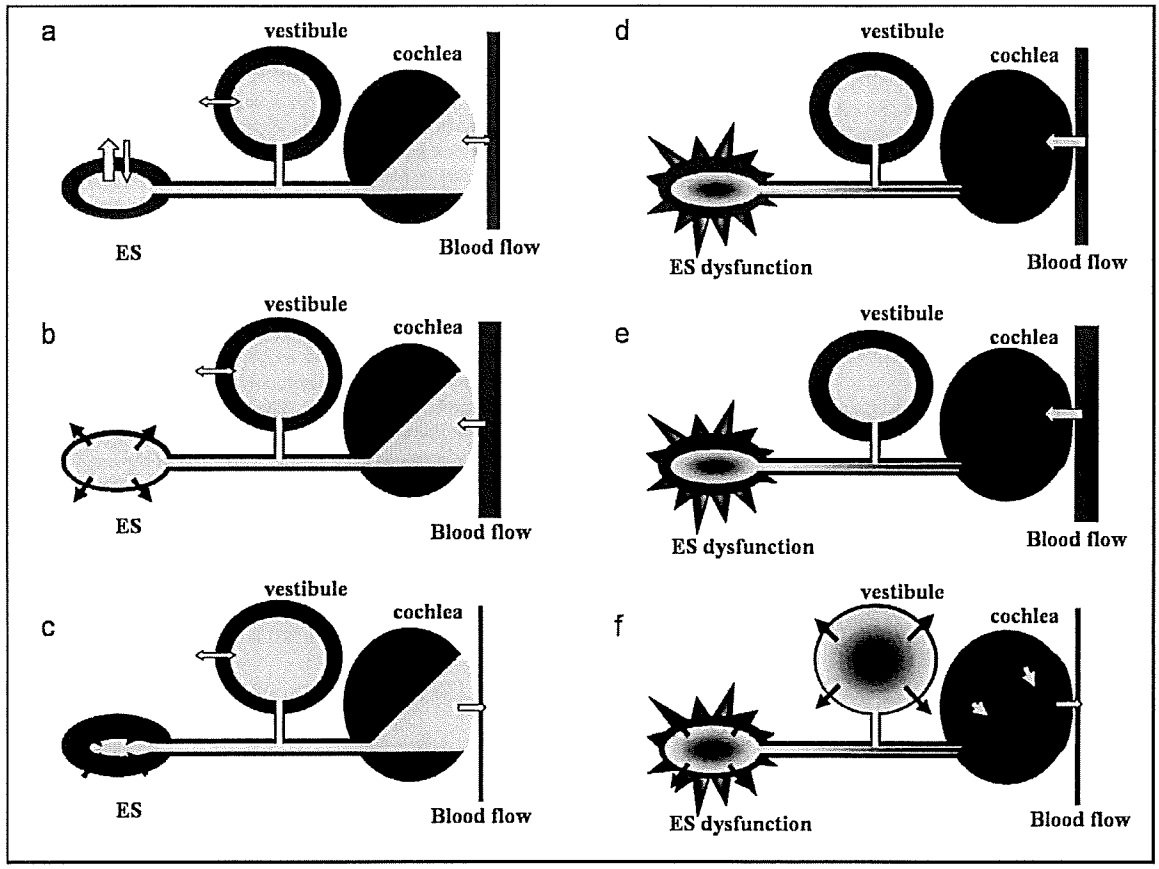


Figure 8. Schematic representation of inner ear blood flow (IBF) changes in the normal (a, b, c) and model animals (d, e, f). (a) Inner ear fluid homeostasis, strictly regulated in normal animals. (b) When the IBF was increased, the endolymphatic volume increased, regulated by the expansion of endolymphatic sac (ES) lumen. (c) When the IBF was reduced, the endolymphatic volume decreased, regulated by the collapse of the ES lumen and subsequent secretion of stainable substance. (d) Model animal, showing endolymphatic hydrops (EH) and ES dysfunction, but no signs of vertigo. (e) When the IBF was increased in the model animals, there were no obvious changes in the inner ear. (f) When the IBF was decreased in the model animals, the volume of endolymph in the cochlea was reduced, resulting in folding of Reissner's membrane. The vestibular part represents the increased EH, which may cause the rapid ionic imbalance resulting in the marked vestibular dysfunction. The ES also shows an abnormal reaction, denoting expansion of the ES lumen.

Chemical factors characteristically include osmotic and hydrostatic pressure changes and, most likely, changes in membrane permeability, causing egress of inappropriate ions through the membrane barrier and consequently affecting sensory dendrites, leading to cochlear and vestibular symptoms.

In conclusion, ES reacts to changes in the IBF, fluid volume, and/or pressure, which may play a certain role in inner ear fluid homeostasis. When this function of the ES is disrupted, additional stress can induce inner ear dysfunction. Further investigation is necessary to elucidate the regulatory mechanisms of IBF as well as inner ear fluid homeostasis, which will assist our understanding and treatment of MD.

## Acknowledgements

This study was supported by a Health and Labor Science Research Grant for Research on Specific Disease (Vestibular Disorders) from the Ministry of Health, Labor and Welfare, Japan (2008), a Grant-in-Aid for Scientific Research (19591972) provided by the Ministry of Education, Science and Culture, Japan and also by the Swedish Medical Research Council (grant no. 17X-7305) and the Foundation Tysta Skolan.

***Declaration of interest:*** The authors report no conflicts of interest. The authors alone are responsible for the content and writing of the paper.

## References

[1] Manchini F, Catalani M, Carru M, Monti B. History of Meniere's disease and its clinical presentation. Otolaryngol Clin North Am 2002;35:565–80.

[2] Kimura RS, Schuknecht H. Membranous hydrops in the inner ear of the guinea pig after the obliteration of the endolymphatic sac. Pract Otorhinolaryngol 1965;27:343–54.

[3] Semaan MT, Alagramam KN, Megerian CA. The basic science of Ménière's disease and endolymphatic hydrops. Curr Opin Otolaryngol Head Neck Surg 2005;13:301–7.

[4] Gates GA. Meniere's disease Review 2005. J Am Acad Audiol 2006;17:16–26.

[5] Dunnebier EA, Segenhout JM, Wit HP, Albers FWJ. Two-phase endolymphatic hydrops: a new dynamic guinea pig model. Acta Otolaryngol 1997;117:13–9.

[6] Kimura RS. Animal models of endolymphatic hydrops. Am J Otolaryngol 1982;3:447–51.

[7] Feldman AM, Brusilow SW. Effects of cholera toxin on cochlear endolymph production: model for endolymphatic hydrops. Proc Natl Acad Sci U S A 1976;73:1761–4.

[8] Takeda T, Takeda S, Kitano H, Okada T, Kakigi A. Endolymphatic hydrops induced by chronic administration of vasopressin. Hear Res 2000;140:1–6.

[9] Tomiyama S. Development of endolymphatic hydrops following immune response in the endolymphatic sac of the guinea pig. Acta Otolaryngol 2004;124:1145–8.

[10] Takumida M, Akagi N, Anniko M. A new animal model for Ménière's disease. Acta Otolaryngol 2008;128:263–71.

[11] Akagi N, Takumida M, Anniko M. Effects of inner ear blood flow changes to the endolymphatic sac. Acta Otolaryngol 2008 (in press).

[12] Kakigi A, Takeda S, Takeda T, Sawada S, Azuma H, Higashiyama K, et al. Time course of dehydrating effects of isosorbide on experimentally induced endolymphatic hydrops in guinea pig. ORL J Otorhinolaryngol Relat Spec 2004;66:291–6.

[13] Hallpike CS, Cairns H. Observation on the pathology of Ménière's syndrome. Proc R Soc Med 1938;31:1317–31.

[14] Yamakawa K. ber die pathologische Veränderung bei einem Meniere-Kranken. Proc 42nd Ann Meet Oto-Rhino-Laryngol Soc Japan J Otolaryngol 1938;44:2310–2.

[15] Paparella MM, Djalilian HR. Etiology, pathophysiology of symptoms, and pathogenesis of Meniere's disease. Otolaryngol Clin North Am 2002;35:529–45.

[16] Takumida M, Bagger-Sjöbäck D, Rask-Andersen H. The endolymphatic sac and inner ear homeostasis. I: Effect of glycerol on the endolymphatic sac with or without colchicine pretreatment. Hear Res 1989;40:1–16.

[17] Takumida M. Dynamic properties of the endolymphatic sac. A morphological and histochemical analysis of secretory and absorptive mechanisms. Thesis, Stockholm, 1989.

[18] Takumida M, Hirakawa K, Harada Y. Effect of glycerol on the guinea pig inner ear after removal of the endolymphatic sac. ORL J Otorhinolaryngol Relat Spec 1995;57:5–9.

[19] Miller JM, Ren T-Y, Nuttall AL. Studies of inner ear blood flow in animals and human beings. Otolaryngol Head Neck Surg 1995;112:101–13.

[20] Ohlsén KA, Didier A, Baldwin D, Miller JM, Nuttall AL, Hultcrantz E. Cochlear blood flow in response to dilating agents. Hear Res 1992;58:19–25.

*Acta Oto-Laryngologica*, 2009; 129: 1340–1350

informa
healthcare

ORIGINAL ARTICLE

# Age-dependent changes in the expression of klotho protein, TRPV5 and TRPV6 in mouse inner ear

MASAYA TAKUMIDA[1], TAKUYA ISHIBASHI[1], TAKAO HAMAMOTO[1], KATSUHIRO HIRAKAWA[1] & MATTI ANNIKO[2]

[1]*Department of Otolaryngology, Hiroshima University Faculty of Medicine, Hiroshima, Japan and* [2]*Department of Otolaryngology, Head and Neck Surgery, University Hospital, Uppsala, Sweden*



**Abstract**

*Conclusions.* klotho protein content decreases with increasing age, which weakens resistance to oxidative stress, resulting in induced cell death as well as modulating endolymph fluid homeostasis. Down-regulation of klotho also leads to down-regulation of TRPV5 and TRPV6, resulting in modified $Ca^{2+}$ homeostasis in the inner ear, dysfunction of sensory cell transduction and causing hearing loss and/or vestibular disorders. *Objective.* Expression of klotho, TRPV5 and TRPV6 in the mouse inner ear and age-related changes were analysed. *Materials and methods.* CBA/J mice aged 8 weeks and 24 months were used in this study. The localization of klotho, TRPV5 and TRPV6 in the inner ear of young and old mice was investigated by immunohistochemistry. *Results.* Immunostaining for klotho was observed in stria vascularis, outer and inner hair cells (OHCs and IHCs), and in vestibular sensory cells and dark cells, and less intensely in the spiral and vestibular ganglion cells. Expression of TRPV5 was found in stria vascularis, organ of Corti, vestibular sensory cells and dark cells, and less intensely in the spiral and vestibular ganglion cells. Expression of TRPV6 was found in supporting cells of the organ of Corti, with weak labelling in OHCs and IHCs. Weak fluorescence was also noted in stria vascularis, and faint fluorescence in the spiral ligament. Vestibular sensory and dark cells as well as vestibular ganglion cells showed weak fluorescence. In the old animals, the expression patterns of klotho, TRPV5 and TRPV6 were identical with those in young animals, although fluorescence intensity was significantly weaker.

**Keywords:** *klotho, TRPV5, TRPV6, inner ear, mouse, ageing, immunohistochemistry*

## Introduction

During the mammalian lifespan, significant changes occur in hearing and/or balance. The sensorineural hearing loss and/or vestibular disorders peculiar to elderly humans are considered to be a consequence of ageing. The mammalian inner ear loses its sensory cells with advancing age, accompanied by a functional deterioration in hearing and balance. Recent studies have demonstrated the presence of various reactive oxygen species (ROS) and different time courses of oxidative changes in individual tissues of the ageing inner ear. An imbalance in redox status may be one component of age-related hearing loss and vertigo [1].

Ageing progresses so slowly and ageing-associated phenomena are so complex that researchers find it difficult to study the molecular mechanisms of this process. However, important findings have come to light thanks to molecular genetic technology. In a recently devised murine model, klotho-deficient mice proved useful for the study of a previously unknown significant pathway responsible for the premature ageing-like phenotype that is exhibited by the mouse mutant [2,3]. The klotho mouse is a recently developed model exhibiting phenotypes resembling those of human ageing, including such age-related ailments as arteriosclerosis, osteoporosis, infertility, age-related skin changes, ectopic calcification and pulmonary emphysema. The cause of these manifestations is a single mutation in what is termed the klotho gene [2,3]. Normally, klotho protein acts in a prophylactic manner in the cardiovascular system by stimulating endothelium-derived nitric

Correspondence: Masaya Takumida MD, Department of Otolaryngology, Hiroshima University Faculty of Medicine, 1-2-3 Kasumicho, Minamiku, Hiroshima 734-8551, Japan. E-mail: masati@hiroshima-u.ac.jp

*(Received 18 December 2008; accepted 7 January 2009)*


print/ISSN 1651-2251 online 
016480902725254

oxide (NO) production via a humoral route. Furthermore, it is abundant in the kidney, where its expression is down-regulated by protracted circulatory stress, such as that associated with long-term hypertension, diabetes mellitus and chronic renal failure, as well as by acute inflammatory stress [2,3].

In the inner ear, klotho gene transcription and protein synthesis have been demonstrated by means of RT-PCR, western blotting and immunohistochemical staining [4]. klotho protein was found mainly in stria vascularis and the spiral ligament, probably modulating ion transport. The threshold for the auditory brainstem response was significantly higher in klotho mice than in wild-type mice, and wave I latencies were prolonged. On the other hand, klotho mice exhibited a normal range of I–IV interpeak intervals. No obvious morphological abnormalities were detected in klotho mice, even though expression of klotho protein was not detected, and there was an obvious hearing disorder. Taken together, these findings suggest that by helping maintain ion homeostasis in the endolymph, klotho protein serves as a key mediator of auditory function [4].

In addition to klotho, inner ear fluid homeostasis is also maintained by a number of mechanisms. For example, the TRPV (transient receptor potential vanilloid) ion channel family is known to play an important part in inner ear sensory transduction and fluid homeostasis. TRPV1 was identified in the organ of Corti and inner ear ganglion cells and TRPV4 was found in the organ of Corti, spiral ganglion cells, stria vascularis, the vestibular sensory cells, vestibular ganglion cells and in the endolymphatic sac [5]. More recently, TRPV2 and TRPV3 were also found in the mouse inner ear, often co-localized with TRPV1 [6]. The functional properties of TRPV1-4 are considered to play a functional role in sensory cell physiology and TRPV4 and TRPV2 play an important role in fluid homeostasis in the inner ear [5,6]. TRPV5 and TRPV6 have also been reported to exist in the inner ear, particularly in stria vascularis and vestibular dark cells [7,8]. The endolymphatic $Ca^{2+}$ concentration is unusually low for an extracellular fluid, which is critically important for sensory transduction. Reabsorption of $Ca^{2+}$ from endolymph has recently been shown to involve the epithelial $Ca^{2+}$ channels TRPV5 and TRPV6. These are inhibited by an acidification of extracellular pH, leading to inhibition of sensory transduction by inhibition of $Ca^{2+}$ absorption and an increase in endolymphatic $Ca^{2+}$ concentration [7,8].

Recently, it was shown that klotho, which strengthens resistance to oxidative stress-induced cell death, is known to diminish with increasing age [9]. TRPV5 is known to be regulated by klotho [10,11]. Moreover, expression of TRPV5 and TRPV6 decreased with increasing age in the renal and intestinal epithelium [12]. This down-regulation of TRPV5 and TRPV6 is probably involved in the impaired $Ca^{2+}$ (re)absorption during ageing. Taken together, these findings strongly suggest that klotho, TRPV5 and TRPV6 may be closely related to the ageing phenomena of the inner ear.

The purpose of this study was to elucidate the expression of klotho protein, TRPV5 and TRPV6 in the inner ear as well as how they change with ageing, in order to reveal the functional properties of klotho, TRPV5, TRPV6 in the inner ear and to improve our understanding of the mechanisms of ageing of the inner ear.

## Materials and methods

We used 10 healthy, otomicroscopically normal, 8-week-old (young) CBA/J mice with body weights in the range 20–25 g and a normal Preyer's reflex and 24-month-old (old) CBA/J mice with body weights in the range 30–35 g. Care and use of the animals was approved by the Animal Experimentation Committee, Hiroshima University School of Medicine (permit no. A06-149) and was in accordance with the Guide to Animal Experimentation, Hiroshima University and the guidelines of the Committee on Research Facilities for Laboratory Animal Science, Hiroshima University School of Medicine.

The young and old animals were deeply anaesthetized with pentobarbital and fixed by cardiac perfusion with 4% paraformaldehyde in 0.1 M phosphate buffer solution, pH 7.4. The temporal bones were excised and immersed in the same fixative for a further 1 h, then decalcified with 0.1 M buffered Na-EDTA for 14 days. The specimens for the light microscopic studies were dehydrated with a graded series of ethanols and embedded in a water-soluble resin (JB-4®). Sections were cut about 4 μm thick and stained with toluidine blue for light microscopy.

The specimens for the immunohistochemical studies were cryoprotected in cold 20% sucrose in phosphate-buffered saline (PBS), frozen in OCT mounting medium (Sakura Finetechnical Co. Ltd, Tokyo, Japan), serially sectioned on a cryostat at 4 μm, and mounted on glass slides. After pretreatment with blocking serum, the specimens were incubated with a goat polyclonal antibody to klotho (R&D Systems, Minnesota, USA) diluted 10 μg/ml, a rabbit polyclonal antibody to TRPV5 or TRPV6 (Osenses Pty Ltd, SA, Australia) at 10 μg/ml dilution, a rabbit polyclonal antibody to nitrotyrosine (Upstate, NT, USA) at a dilution of 10 μg/ml, a

rabbit polyclonal antibody to hydroxynonenal (Alexis Biochem, Lausanne, Switzerland) diluted 1:500 or with a goat polyclonal antibody to superoxide dismutase 2 (SOD2) (Santa Cruz Biotechnology, CA, USA) diluted 1:100 in 0.3% Triton X100 containing PBS at 4°C for 48 h. The specimens were then washed in PBS and incubated for 1 h with Alexa Fluor 488 goat anti-rabbit or donkey anti-goat secondary antibodies (1:500) (Molecular Probes, Eugene, OR, USA). The sections were washed and coverslipped with DakoCytomatia Fluorescent Mounting Medium (DakoCytomatia, CA, USA). The specimens were viewed in a Nikon fluorescence microscope (Eclipse E600) equipped with an appropriate filter set. Fluorescence analogue images were obtained via an intensified digital colour charge-coupled device camera (C4742-95; Hamamatsu Photonics) and stored as digital images using IP Lab Spectrum software (version 3.0; Signal Analytics Corporation).

*Measurement of fluorescence intensities*

For the statistical analysis, we compared the fluorescence intensity in young vs old animals in the different parts, i.e. stria vascularis, outer hair cells (OHCs), spiral ganglion cells, vestibular hair cells (VHCs), dark cells and vestibular ganglion cells. The sensory cells, ganglion cells, dark cells, and cells in stria vascularis were randomly selected from each specimen, and their fluorescence intensity was measured. The values of 10 cells were averaged for each specimen. Grand means were obtained by averaging the means of six to eight specimens for young and for old animals. A standard error was calculated from the means for individual specimens. These data were analysed by two-way analysis of variance (ANOVA). To visualize fluorescence intensity, some pictures were depicted in pseudocolour using IP Lab Spectrum software; purple represented intense fluorescence and red represented weak fluorescence.

## Results

*Light microscopy*

In the old animals, the organ of Corti showed degeneration such as flattening and distortion of the organ, occasionally with loss of hair cells. Strial atrophy appeared as sporadic thinning that occurred throughout the cochlear turns, often reducing the light microscopic appearance of the stria to a single cellular layer. Other associated changes included cystic degeneration of strial elements and atrophy of the spiral ligament. Loss of spiral ganglion cells, with a relative sparing of the organ of Corti, was also observed (Figure 1). In the vestibular end organs, loss of sensory cells was observed but was less severe than that in the organ of Corti. The otoconial layer became thinner and vestibular ganglion cells were fewer (Figure 2).

*Expression of hydroxynonenal, nitrotyrosine and SOD2*

Immunofluorescence for both hydroxynonenal (HNE) and nitrotyrosine (NT) was observed in

Figure 1. (a) Cochlea of the young animal. (b) In the old animals, the organ of Corti shows degeneration, with loss of hair cells (arrow). Strial atrophy appears as a sporadic thinning, with atrophy of the spiral ligament (arrowhead). (c) Spiral ganglion of young animal. (d) A loss of spiral ganglion cells is evident in old animals.

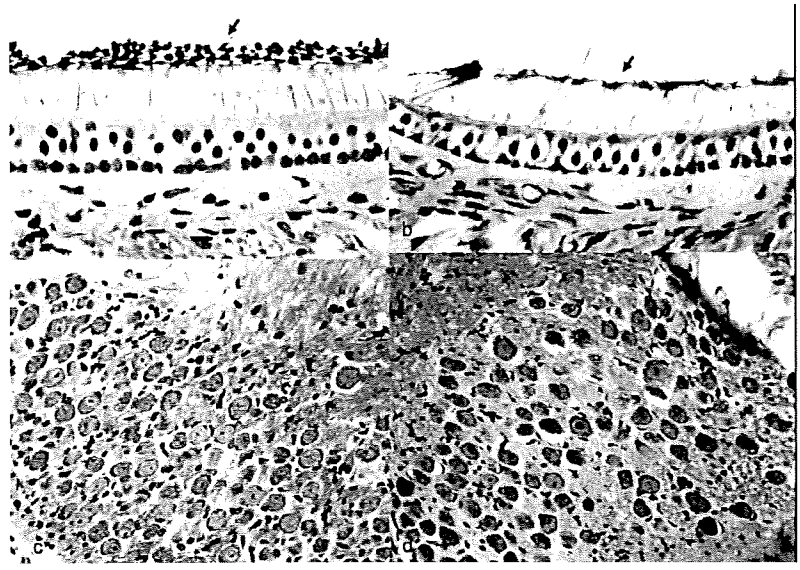

Figure 2. (a) Utricular macula of young animal. Arrow, otoconia. (b) In the utricle of old animals, loss of hair cells is evident, but not so severe as that of the organ of Corti. The otoconial layer becomes thinner (arrow). (c) Vestibular ganglion of young animal. (d) Vestibular ganglion cells are fewer in old animals.



all cell types of the organ of Corti, but was weak in the 8-week-old mice. Immunofluorescence was stronger at 24 months, especially in the area of the phalangeal processes of Deiters' cells and the inner and outer pillar cells. In the spiral ganglion cells, immunofluorescence was again weak at 8 weeks and more intense at 24 months. A similar temporal pattern of fluorescence for both HNE and NT was seen in stria vascularis. In the vestibular end organs, immunofluorescence for HNE and NT was observed in the sensory and vestibular dark cells and also in the vestibular ganglion cells. This fluorescence was more intense in the old mice (Figure 3).

Immunofluorescence for SOD2 was detected in the cochlea of the young animals. Stria vascularis showed marked immunoreactivity to SOD2. Strong-to-moderate fluorescence was observed in the organ of Corti. Moderate-to-weak fluorescence was observed in the stroma of the spiral limbus and in spiral ganglion cells. At the age of 24 months, immunoreactivity to SOD2 decreased in the organ of Corti and in stria vascularis. In the spiral ganglion cells, immunostaining decreased in the old animals as well (Figure 4). In the vestibular end organs, immunofluorescence for SOD2 in the young animals was observed mainly in the dark cells, with weaker staining in the sensory and vestibular ganglion cells, significantly decreased in the old animals.

*Expression of klotho protein*

Immunostaining for klotho in the inner ear revealed the presence of klotho protein in the lateral wall of the cochlear duct and within stria vascularis. The latter was intensely labelled, while the spiral prominence and ligament showed slight labelling. In the organ of Corti, OHCs, IHCs and some supporting cells showed intense fluorescence, while spiral ganglion cells revealed weaker staining. In the vestibule, vestibular sensory cells and dark cells showed intense immunofluorescence, while the vestibular ganglion cells revealed weaker fluorescence. In the old animals, the expression patterns were identical to those of the young animals, whereas fluorescence was significantly weaker (Figure 5).

*Expression of TRPV5 and TRPV6*

Expression of TRPV5 was found mainly in marginal cells of the stria vascularis and organ of Corti (Figure 6), while weaker staining was noted in the spiral ganglion cells (Figure 7). Vestibular sensory cells and dark cells also showed immunofluorescence, with weaker labelling in the vestibular ganglion cells (Figure 7). Expression of TRPV6 was observed mainly in supporting cells of the organ of Corti, with weaker labelling in OHCs and IHCs. Weaker fluorescence was noted in the stria vascularis and faint fluorescence in the spiral ligament (Figure 6). Vestibular sensory and dark cells also showed weak fluorescence (Figure 7), as did the vestibular

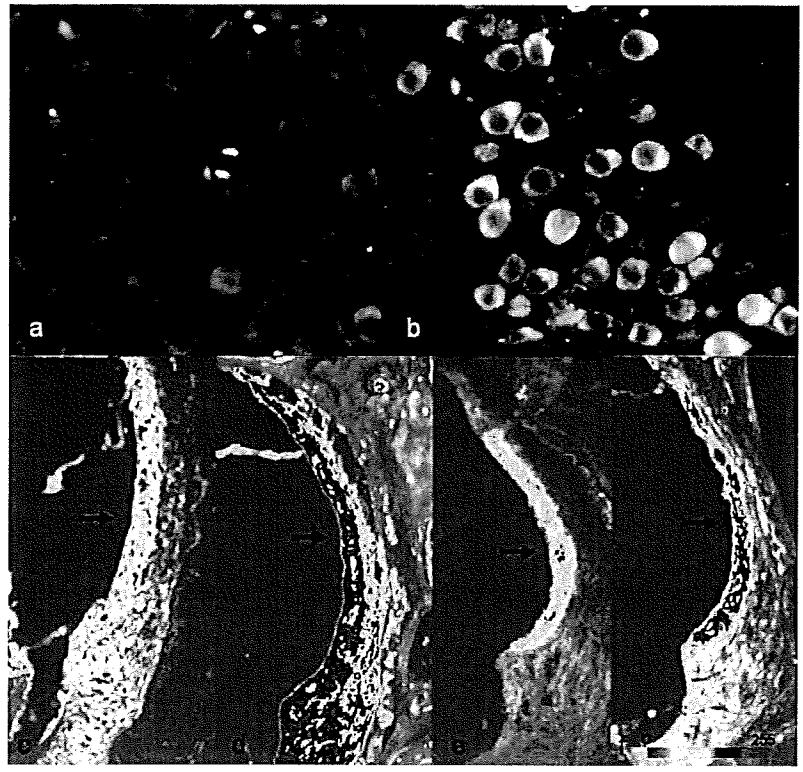


Figure 3. Staining for HNE is present in spiral ganglion cells but remains weak at the age of 8 weeks (a). Staining intensifies at 24 months (b). Staining for both HNE (c) and NT (e) is weak in stria vascularis. Staining intensifies at 24 months: d) HNE; (f) NT.

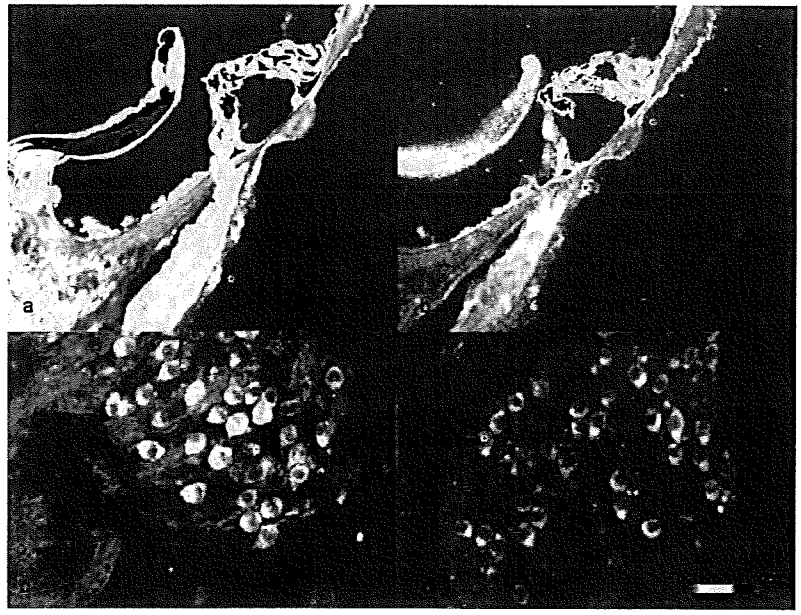


Figure 4. Immunostaining for SOD2 in young organ of Corti (a) and spiral ganglion cells (c) indicating presence of SOD. At the age of 24 months, immunofluorescence has decreased (b, d).

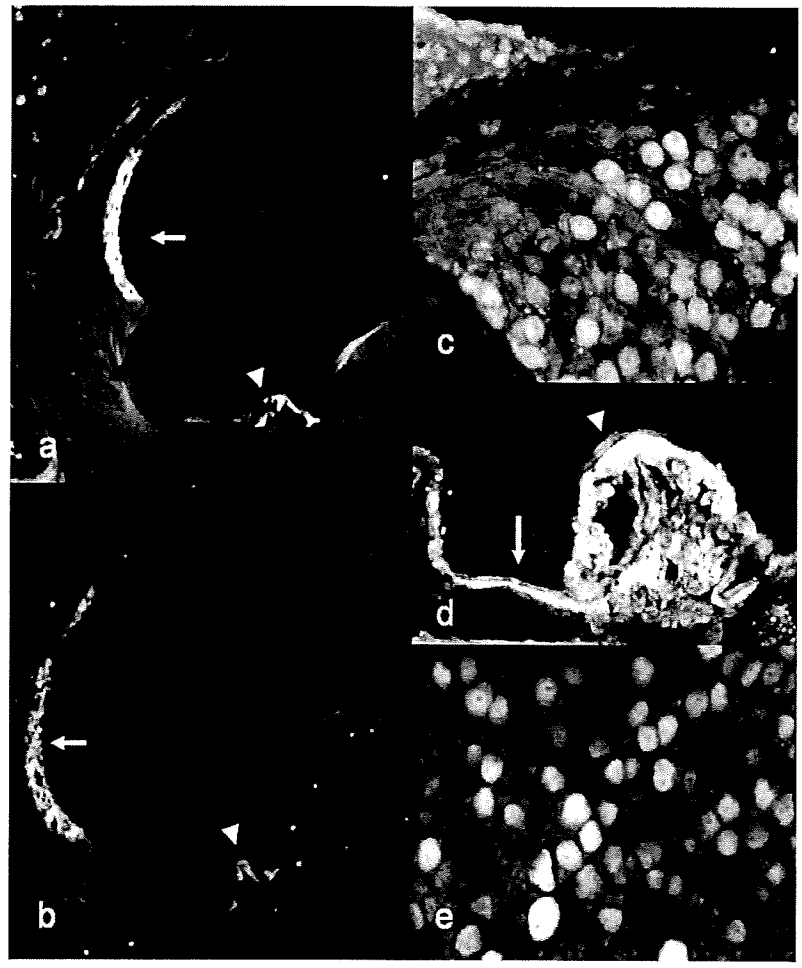


Figure 5. (a) Immunostaining for klotho in inner ear reveals the presence of klotho protein in stria vascularis (arrow). In the organ of Corti (arrowhead), OHCs, IHCs and some supporting cells display intense fluorescence, while spiral ganglion cells (c) show weaker staining. In the vestibule, vestibular sensory cells (arrowhead) and dark cells (arrow) display intense immunofluorescence (d), while vestibular ganglion cells show weaker fluorescence (e). In old animals, fluorescence intensity was significantly reduced (b) (arrowhead, organ of Corti; arrow, stria vascularis).

ganglion cells. In the old animals, the expression patterns of TRPV5 and TRPV6 were identical to those of young animals, but fluorescence intensity was significantly weaker (Figure 6).

*Changes in expression of klotho, TRPV5 and TRPV6 in young and old animals*

The expression patterns of klotho, TRPV5 and TRPV6 in the inner ears of 24-month-old mice were identical to those in 8-week-old mice, but fluorescence intensity was weaker in the old animals. The fluorescence intensity of klotho in the young mice was $138 \pm 31.1$ (mean$\pm$SD) in OHCs, $82 \pm 10.9$ in spiral ganglion cells, $134 \pm 20.1$ in stria vascularis, $132 \pm 13.3$ in VHCs of crista ampullaris, $170 \pm 33.4$ in vestibular dark cells and $68 \pm 6.1$ in vestibular ganglion cells. In the old mice, fluorescence intensity decreased significantly to $105 \pm 10.5$ in OHCs ($p < 0.05$), $70 \pm 4.2$ in spiral ganglion cells ($p < 0.01$), $79 \pm 13.8$ in stria vascularis ($p < 0.01$), $90 \pm 13.8$ in VHCs ($p < 0.01$), $74 \pm 15.3$ in dark cells ($p < 0.01$) and $56 \pm 9.4$ in vestibular ganglion cells ($p < 0.01$) (Figure 8).

Fluorescence intensity of TRPV5 in the young mice was $135 \pm 31.4$ in OHCs, $82 \pm 12.6$ in spiral ganglion cells, $77 \pm 7.0$ in stria vascularis, $152 \pm 15.4$ in VHCs, $135 \pm 15.5$ in dark cells and $74 \pm 9.1$ in vestibular ganglion cells. In the old mice, fluorescence intensity decreased significantly to $92 \pm 10.1$ in OHCs ($p < 0.01$), $68 \pm 17.6$ in spiral ganglion cells ($p < 0.01$), $45 \pm 3.1$ in stria vascularis ($p < 0.01$), $132 \pm 5.7$ in VHCs ($p < 0.05$), $120 \pm 5.7$ in dark cells ($p < 0.05$) and $43 \pm 2.9$ in vestibular ganglion cells ($p < 0.01$) (Figure 8).

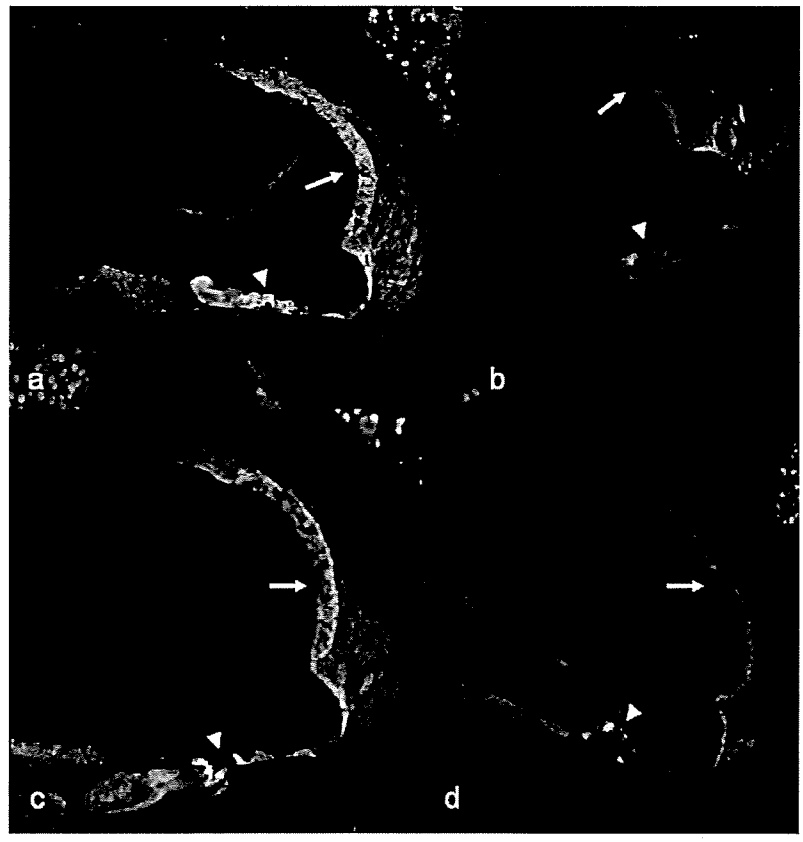


Figure 6. (a) Expression of TRPV5, mainly in marginal cells of stria vascularis (arrow) and organ of Corti (arrowhead). (c) Expression of TRPV6 found mainly in supporting cells of organ of Corti (arrowhead), with weaker labelling in OHCs and IHCs. Weaker fluorescence is noted in stria vascularis (arrow), and faint fluorescence in the spiral ligament. In the old animals, the expression patterns of TRPV5 (b) and TRPV6 (d) are identical to those of young animals, while the fluorescence intensity is significantly reduced (arrowhead, organ of Corti; arrow, stria vascularis).

Fluorescence intensity of TRPV6 in the young mice was $119 \pm 17.7$ in OHCs, $76 \pm 17.4$ in spiral ganglion cells, $53 \pm 5.8$ in stria vascularis, $148 \pm 15.0$ in VHCs, $90 \pm 9.4$ in dark cells and $65 \pm 8.5$ in vestibular ganglion cells. In the old mice, fluorescence intensity decreased significantly to $73 \pm 12.5$ in OHCs ($p < 0.01$), $58 \pm 8.3$ in spiral ganglion cells ($p < 0.01$), $38 \pm 1.8$ in stria vascularis ($p < 0.01$), $125 \pm 14.9$ in VHCs ($p < 0.01$), $68 \pm 8.7$ in dark cells ($p < 0.05$) and $43 \pm 2.1$ in vestibular ganglion cells ($p < 0.01$) (Figure 8).

## Discussion

The klotho gene was recently shown to be involved in suppressing several phenotypes associated with ageing; indeed, its disruption in mice resulted in a syndrome strongly resembling human ageing [2,3]. klotho is expressed predominantly in tissues involved in regulating $Ca^{2+}$ homeostasis, including the distal convoluted tubules (DCTs) in the kidney as well as parathyroid hormone-secreting cells and the epithelium of the choroid plexus in the brain. klotho proteins have been predicted to be present on the cell surface of klotho-expressing cells, as the klotho gene encodes a type a membrane protein. However, a large amount of klotho is present in the cytoplasm. The involvement of klotho in regulating $Ca^{2+}$ homeostasis is consistent with its predominant expression in kidney DCTs, in parathyroid glands, and in the choroid plexus in the brain, all of which are indispensable for the regulation of calcium homeostasis. It has been reported that klotho activates the TRPV5 by hydrolysing the extracellular N-linked oligosaccharide of this receptor. TRPV5, klotho and calbindin-$D_{28K}$ (the vitamin D-sensitive intracellular $Ca^{2+}$ transporting protein) are exclusively co-expressed in DCT cells, which form the nephron segments responsible for the active and regulated transepithelial $Ca^{2+}$ reabsorption in the kidney. This finding suggests the importance of these klotho/TRPV5/calbindin-$D_{28K}$ positive cells and the substantial biological roles of klotho and TRPV5 proteins in the regulation of $Ca^{2+}$

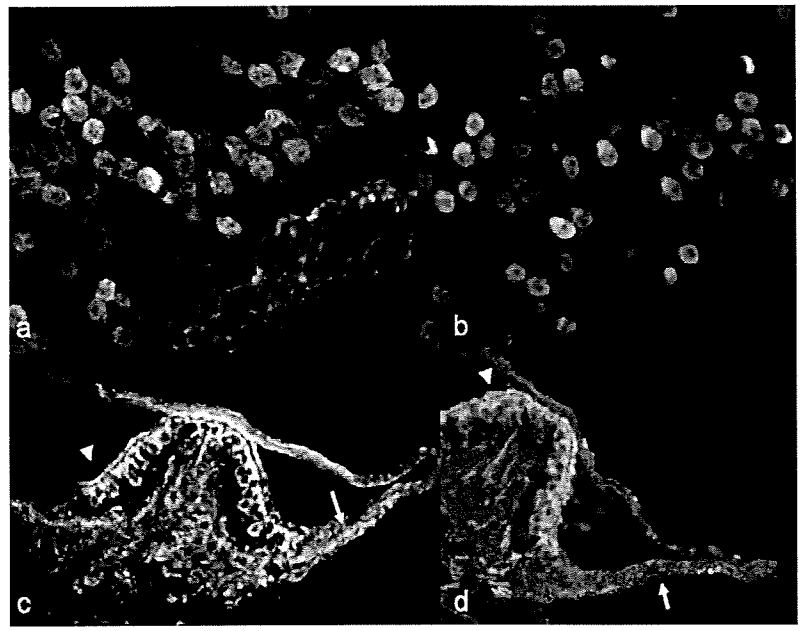


Figure 7. Immunofluorescence for TRPV5 (a) and TRPV6 (b) noted in spiral ganglion cells. Vestibular sensory cells (arrowheads) and dark cells (arrow) show immunofluorescence for TRPV5 (c) and TRPV6 (b). (d) Combined image of fluorescence for TRPV6 and bright field.



homeostasis [11]. Consistently, mice lacking TRPV5 suffer from diminished renal $Ca^{2+}$ reabsorption, causing severe hypercalciuria and compensatory hyperabsorption of dietary $Ca^{2+}$ in the intestines. It has therefore been speculated that klotho deficiency may cause down-regulation of TRPV5 and impair calcium balance, even when the overproduction of vitamin D is rescued by diet or genetic manipulation [3].

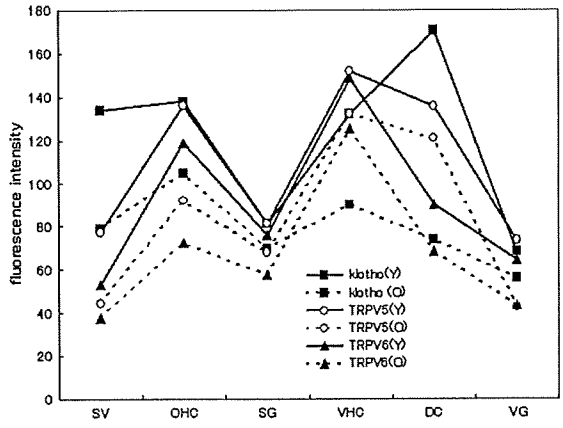


Figure 8. Changes in expression of klotho, TRPV5 and TRPV6 in young (Y) vs old (O) animals. The fluorescence intensity of klotho, TRPV5 and TRPV6 is significantly weaker in the old animals. SV, stria vascularis; OHC, outer hair cells; SG, spiral ganglion cells; VHC, vestibular hair cells; DC, vestibular dark cells; VG, vestibular ganglion cells

In the inner ear, a recent study has indicated a substantial presence of klotho in the stria vascularis of mice [4]. The present study also revealed the expression of klotho in stria vascularis as well as in the vestibular dark cells. These sites are regarded as fluid-transporting cells in the inner ear, which regulate inner ear fluid homeostasis. Co-expression of klotho and TRPV5 in stria vascularis and the vestibular dark cells was also demonstrated in this study. Based on these findings, it is readily speculated that klotho and TRPV5 play an important role in regulating calcium homeostasis in the inner ear.

Another function of klotho has also been suggested. Stria vascularis is known to be a key regulator of $K^+$ secretion into and $Na^+$ absorption from the endolymph, thereby maintaining its ionic composition and generating the endocochlear potential [13]. The distribution of klotho protein and Na-K-Cl co-transporter is similar in stria vascularis, which suggests that klotho participates in regulating the ionic composition of the endolymph.

The present study revealed that klotho protein is also expressed in the inner ear sensory transduction systems, i.e. OHCs and IHCs, spiral ganglion cells, VHCs and vestibular ganglion cells. Thus, klotho seems closely related to inner ear sensory cell transduction. Although the physiological functions of klotho protein and the mechanisms regulating klotho gene expression remain unclear, changes in klotho gene expression are involved in hearing and/or balance impairment.

The TRPV family comprises six mammalian members: TRPV1–TRPV6. Members of the TRPV family contain three to five ankyrin repeats in their cytosolic $NH_2$ termini. TRPV1–TRPV4 are all heat-activated channels that are non-selective for cations and modestly permeable to $Ca^{2+}$. The properties of the other two members of this subfamily, TRPV5 and TRPV6, are quite different from those of TRPV1–TRPV4. They are the only highly $Ca^{2+}$-selective channels in the TRP family, and both are strictly regulated by intracellular $Ca^{2+}$. Under physiological conditions, these channels exclusively conduct $Ca^{2+}$, but in the absence of extracellular $Ca^{2+}$, monovalent cations permeate readily, resulting in anomalous mole fraction behaviour similar to that observed in other types of $Ca^{2+}$-selective channels. These properties allow TRPV5 and TRPV6 to act as gatekeepers (regulators) in epithelial $Ca^{2+}$ transport, and as selective $Ca^{2+}$ influx pathways in non-excitable cells. In contrast to the other TRPVs, the temperature sensitivity of TRPV5 and TRPV6 is minimal [14]. The body is enabled to reabsorb $Ca^{2+}$ quickly and actively when the extracellular $Ca^{2+}$ concentration in the circulation decreases. Epithelial cells are well equipped to transport and sustain a high rate of $Ca^{2+}$ influx. A key factor creating such increased $Ca^{2+}$ influx is to increase TRPV5 and TRPV6 channel abundance at the epithelial cell surface. TRPV5 is expressed in certain tissues such as kidney, placenta and bone, plays a major role in $Ca^{2+}$ transport, and is localized at the apical membrane of epithelial cells or at the ruffled border membrane of osteoclasts. TRPV5 is located in or near the apical membrane in kidney DCTs, whereas in connecting tubules (CNTs) a large subset of TRPV5 is located subapically. Detailed expression and (co)localization studies suggested that TRPV5 comprises the epithelial $Ca^{2+}$ channel predominantly involved in renal transcellular $Ca^{2+}$ transport in DCTs and CNTs, whereas TRPV6 was postulated to mediate duodenal $Ca^{2+}$ absorption [10]. Therefore, it is hypothesized that these channels are transferred from intracellular vesicles into the plasma membrane. Furthermore, high $Ca^{2+}$ influx is obtained by prolonging the channel's existence at the cell surface before inactivation or internalization. Recently, molecular mechanisms of TRPV5/6 inhibition by both intra- and extracellular acidic pH were reported.

In the inner ear, TRPV5 and TRPV6 have been shown in stria vascularis and in semicircular canal ducts of the vestibular system [7,8]. The present study confirmed the expression of TRPV5 and TRPV6 at the same sites. Endolymphatic $Ca^{2+}$ concentration, which is critically important for sensory transduction, was unusually low. Reabsorption of $Ca^{2+}$ from vestibular endolymph was recently shown to involve the epithelial $Ca^{2+}$ channels TRPV5 and TRPV6. These are inhibited by acidification of extracellular pH and transepithelial $Ca^{2+}$ absorption in TRPV5, while TRPV6-expressing rat semicircular canal epithelium was inhibited by extracellular acidification. These findings indicate that part of the vestibular dysfunction, such as observed in Pendred syndrome, may be due to restriction of sensory transduction by inhibition of $Ca^{2+}$ absorption and an increase in endolymphatic $Ca^{2+}$ concentration [8].

In stria vascularis, reabsorption of $Ca^{2+}$ involves apically expressed $Ca^{2+}$ channels TRPV5 and TRPV6 in conjunction with basolaterally expressed $Ca^{2+}$-ATPases and $Na^+/Ca^{2+}$ exchangers. The finding that TRPV5 is expressed in the apical membrane of strial marginal cells, in conjunction with the finding of $Ca^{2+}$-ATPase PMCA1 in their basolateral membrane, confirms that the stria vascularis is involved in $Ca^{2+}$ reabsorption [7]. This applies also in the case of vestibular dark cells. The presence of TRPV5 and TRPV6 in vestibular dark cells indicates their involvement in $Ca^{2+}$ reabsorption and can be one regulator of vestibular calcium homeostasis.

Expression of TRPV5 and TRPV6 is of great interest as these channels are inhibited by extracellular acidification. Endolymphatic acidification can inhibit $Ca^{2+}$ absorption and lead to the observed increase in endolymphatic $Ca^{2+}$ concentration [7,8]. The present study found that TRPV5 and TRPV6 are expressed in both the organ of Corti and the vestibular sensory cells. Most $Ca^{2+}$ that enters the hair cell bundle via the transduction channel under physiological conditions is extruded by $Ca^{2+}$-ATPases that are expressed in that bundle [15]. Although $Ca^{2+}$ is necessary to maintain the sensitivity of the bundle by adaptation and motility [16], entry of excess $Ca^{2+}$ into the sensory cells leads to $Ca^{2+}$ overloading and cell death. The ability of cochlear hair cells to extrude $Ca^{2+}$ is likely to be limited, especially in OHCs, which do not appear to express plasma membrane $Ca^{2+}$-ATPases in their basolateral membrane [17]. $Ca^{2+}$ overload can be a reason for the cellular degeneration that was observed to begin with OHCs between P7 and P15 [7]. It has therefore been proposed that TRPV5 and TRPV6 also play an important role in calcium homeostasis in the inner ear sensory cells including sensory transduction.

Our study showed that the expression of klotho protein in the inner ear is reduced in old animals. The activity of antioxidant enzymes decreased with advancing age [1,9]. We also showed that in the old animals, expression of SOD2 decreased in inverse

proportion to the increased expression of HNE and NT, as was reported previously [1]. On the other hand, the concentration of the age-related gene, klotho, is known to decrease with advancing age. Expression of klotho is closely related to the lifespan of the organism. Recently, it was shown that klotho increases the organism's resistance to oxidative stress-induced cell death [9]. Thus, our findings may indicate that the age-related decrease in klotho weakens the resistance to oxidative stress.

Similarly, TRPV5 and TRPV6 are also known to decrease with advancing age. Intestinal $Ca^{2+}$ absorption was decreased by ageing, especially its active transport by the duodenum. Furthermore, similar age-related changes take place in the kidney. In mice, ageing resulted in a tendency to increased renal $Ca^{2+}$ excretion and significantly reduced intestinal $Ca^{2+}$ absorption, which was accompanied by reduced expression of TRPV5 and TRPV6, respectively, despite elevated serum $1,25(OH)_2D_3$ levels. It is therefore concluded that down-regulation of TRPV5 and TRPV6 is probably involved in the impaired $Ca^{2+}$ (re)absorption during ageing. Age-related decrease takes place in the expression of the key agents responsible for active $Ca^{2+}$ transport, including TRPV5 and TRPV6, and contributes to the decline in intestinal and renal $Ca^{2+}$ (re)absorption with ageing [12]. This may also be the case for the inner ear. For example, the calcium content of otoconia was found to be reduced in old animals [18]. The down-regulation of TRPV5 and TRPV6 in the aged inner ear seems to be related to this phenomenon.

The recent elucidation of a mechanism of TRPV5 regulation by the anti-ageing hormone klotho illustrates the importance of controlling channel abundance at the cell surface. Chang et al. [11] showed that klotho is completely co-localized with TRPV5 at or near the apical membrane in DCTs and CNTs. In addition, it was found that klotho is present in urine, serum and cerebrospinal fluid, as well as in the supernatant obtained from transfected HEK-293 cells expressing klotho, suggesting that it operates from the extracellular space to regulate transcellular $Ca^{2+}$ transport. Expression of TRPV5 and klotho in HEK-293 cells, or direct application of klotho supernatant to TRPV5-expressing HEK-293 cells, stimulated TRPV5-mediated $^{45}Ca^{2+}$ uptake, suggesting a physiological effect of klotho circulating in the bloodstream [10]. Superabundance of klotho in mice significantly extended their lifespan and retarded symptoms of ageing, whereas klotho knockout mice displayed characteristics correlating with premature ageing and the specific pathophysiology of TRPV5 knockout mice (i.e. disturbed $Ca^{2+}$ homeostasis, vitamin D metabolism and bone abnormalities) [3]. Further analysis of the molecular mechanism by which klotho stimulates $Ca^{2+}$ influx included cell surface biotinylation experiments that revealed a significant increase in plasma membrane localization of TRPV5, while at the same time its total expression was not affected following klotho treatment. Interestingly, these effects could be mimicked by a purified β-glucuronidase, indicating that the enzymatic activity of klotho is responsible for the increased TRPV5 activity [10]. Our study revealed the co-expression of klotho and TRPV5 in the inner ear and that fluorescence intensity of both klotho and TRPV5 was reduced in the old animals. Our findings propose that klotho is of importance for regulation of TRPV5 and also seems to be responsible for the reduced TRPV5 activity in old animals.

In conclusion, klotho protein decreases with increasing age, which diminishes the resistance to oxidative stress, causing cell death as well as inducing altered endolymph fluid homeostasis. Down-regulation of klotho also induces the down-regulation of TRPV5 and TRPV6, resulting in altered $Ca^{2+}$ homeostasis in the inner ear and dysfunction of sensory cell transduction and causes hearing loss and/or vestibular disorders.

## Acknowledgements

This study was supported by a Health and Labor Science Research Grant for Research on Specific Disease (Vestibular Disorders) from the Japanese Ministry of Health, Labor and Welfare (2008), a Grant-in-Aid for Scientific Research (19591972) provided by the Ministry of Education, Science and Culture, Japan and also by the Swedish Foundation Tysta Skolan.

***Declaration of interest:*** The authors report no conflicts of interest. The authors alone are responsible for the content and writing of the paper.

## References

[1] Jiang H, Talaska AE, Schacht J, Sha S-H. Oxidative imbalance in the aging inner ear. Neurobiol Aging 2007; 28:1605–12.

[2] Kuro-o M, Matumura Y, Aizawa H, Kawaguchi H, Suga T, Utsugi T, et al. Mutation of the klotho gene leads to a syndrome resembling aging. Nature 1997;390:45–51.

[3] Nabeshima Y-I. Toward a better understanding of klotho. Sci Aging Knowl Environ 2006;8:11.

[4] Kamemori M, Ohyama Y, Kurabayashi M, Takahashi K, Nagai R, Furuya N. Expression of klotho protein in the inner ear. Hear Res 2002;171:103–10.

[5] Takumida M, Kubo N, Ohtani M, Suzuka Y, Anniko M. Transient receptor potential channels in the inner ear: presence of transient receptor potential channel superfamily 1 and 4 in the guinea pig inner ear. Acta Otolaryngol 2005; 125:929–34.

[6] Ishibashi T, Takumida M, Akagi N, Hirakawa K, Anniko M. Expression of transient receptor potential vanilloids 1, 2, 3 and 4 in the mouse inner ear. Acta Otolaryngol 2008;128: 1286–93.

[7] Wangemann P, Nakaya K, Wu T, Maganti RJ, Itza EM, Sanneman JD, et al. Loss of cochlear $HCO_3^-$ secretion causes deafness via endolymphatic acidification and inhibition of $Ca^{2+}$ reabsorption in a Pendred syndrome mouse model. Am J Physiol Renal Physiol 2007;292:F1345–53.

[8] Nakaya K, Harbidge DG, Wangemann P, Schultz BD, Green ED, Wall SM, et al. Lack of pendrin $HCO_3^-$ transport elevates vestibular endolymphatic $[Ca^{2+}]$ by inhibition of acid-sensitive TRPV5 and TRPV6 channels. Am J Physiol Renal Physiol 2007;292:F1314–21.

[9] Shih P-H, Yen G-C. Differential expressions of antioxidant status in aging rats: the role of transcriptional factor Nrf2 and MAPK signaling pathway. Biogerontology 2007;8:71–80.

[10] Schoeber JPH, Hoenderop JGJ, Bindels RJM. Concerted action of associated proteins in the regulation of TRPV5 and TRPV6. Biochem Soc Trans 2007;35(Pt 1):115–9.

[11] Chang Q, Hoefs S, Kemp W, Topala CN, Bindels RJ, Hoenderop JG. The β-glucuronidase klotho hydrolyzes and activates the TRPV5 channel. Science 2005;310:490–3.

[12] Van Abel M, Huybers S, Hoenderop JGJ, van de Kemp AWCM, van Leeuwen JPTM, Bindels RJM. Age-dependent alterations in $Ca^{2+}$ homeostasis: role of TRPV5 and TRPV6. Am J Physiol Renal Physiol 2006;291:F1177–83.

[13] Offner FF, Dallos P, Cheatham MA. Positive endocochlear potential: mechanism of production by marginal cells of stria vascularis. Hear Res 1987;29:117–24.

[14] Nilium B, Owsianik G, Voets T, Peters JA. Transient receptor potential cation channels in disease. Physiol Rev 2007;87:165–217.

[15] Yamoah EN, Lumpkin EA, Dumont RA, Smith PJ, Hudspeth AJ, Gillespie PG. Plasma membrane $Ca^{2+}$-ATPase extrudes $Ca^{2+}$ from hair cell stereocilia. J Neurosci 1998;18: 610–24.

[16] Benser ME, Marquis RE, Hudspeth AJ. Rapid, active hair bundle movements in hair cells from the bullfrog's sacculus. J Neurosci 1996;16:5629–43.

[17] Crouch JJ, Schulte BA. Expression of plasma membrane Ca-ATPase in the adult and developing gerbil cochlea. Hear Res 1995;92:112–9.

[18] Takumida M, Zhang DM. Electron probe X-ray microanalysis of otoconia in guinea pig inner ear: a comparison between young and old animals. Acta Otolaryngol 1997;117: 529–37.